Performance of Joint Detection Techniques for Coded MIMO-OFDM and MIMO-MC-CDM

Markus A. Dangl, Doris Yacoub, Ulrich Marxmeier, Werner G. Teich, Jürgen Lindner
University of Ulm, Dept. of Information Technology
Albert-Einstein-Allee 43, 89081 Ulm, Germany
Email: {markus.dangl,doris.yacoub,ulrich.marxmeier,werner.teich,juergen.lindner}@e-technik.uni-ulm.de

Abstract

We consider a coded transmission over a time-invariant MIMO channel where channel state information is present at the receiver but not at the transmitter. As basic modulation technique we apply OFDM. We investigate the performance of the system when spreading in frequency direction is included additionally (MC-CDM). In the case of MIMO-OFDM crosstalk only occurs because of the use of multiple transmit antennas, whereas MIMO-MC-CDM systems are additionally affected by interference among subcarriers. Therefore, we utilize advanced joint detection techniques with moderate computational complexity like iterative detection, demapping, and decoding to mitigate the interference in both cases.

1. Introduction

Multicarrier (MC) transmission schemes are considered to be promising candidates for the fourth generation of mobile communication systems. A reason lies in the efficient utilization of the available bandwidth, allowing high data rates. Among several MC variants, OFDM represents a well-known technique and is used in broadcast media like, e. g. , European terrestrial digital television (DVB-T) and digital audio broadcasting (DAB), and in wireless local area networks (WLAN), like the IEEE 802.11a standard. However, it may happen that one or more subcarriers of an OFDM system are completely faded out due to the frequency-selective behavior of the channel. Spreading over the subcarriers is a technique to overcome this problem. It was introduced, e. g. , in [1] and is most commonly referred to as MC-CDMA or MC Spread Spectrum [2]. In [3], MC-CDMA is extensively discussed in the context of various multiplexing/multiple access schemes and its advantage over conventional OFDM is shown for both SISO (single input single output) and SIMO (single input multiple output) channels. In the following, we assume a single user system only and therefore use the term MC-CDM (code division multiplexing) rather than MC-CDMA. Furthermore, we include channel coding in the transmission chain to enable a fair comparison between OFDM and MC-CDM.

In order to enhance the bandwidth efficiency and yet maintain high data rates, we consider multiple antennas at both the transmit and receive side [4]. Accordingly, we denote the corresponding OFDM and MC-CDM transmission as MIMO (multiple input multiple output)-OFDM and MIMO-MC-CDM, respectively. Unlike the SIMO case, in a MIMO environment the transmitted symbols are subject to interference for both OFDM and MC-CDM. Therefore, joint detection algorithms are necessary to mitigate the interference. In this paper, we compare the performance of two soft interference cancellation schemes with moderate computational complexity for both coded MIMO-OFDM and MIMO-MC-CDM. One method is based on recurrent neural networks (RNN) which was introduced, e. g. , in [5], extended to complex symbol alphabets in [6] and [7], and to turbo equalization in [8] and [9]. The other detector is denoted as Soft Cholesky Block Decision Feedback Equalizer (SCE) which was introduced for the uncoded case in [10] and for turbo equalization in [11]. We improve the performance of the SCE by including iterative demapping (IDEM) [12] in a turbo scheme. This approach was pursued for an RNN equalizer in [13]. We demonstrate with simulation results that additional spreading in frequency direction improves the bit error rate (BER) performance for most of the applied detection techniques although the level of interference is higher.

2. System Model

In this section, we first introduce an OFDM and MC-CDM system model with one transmit and receive antenna (SISO-OFDM, SISO-MC-CDM) and extend this model to the MIMO case (MIMO-MC-CDM and MIMO-OFDM). We apply a discrete-time vector-valued transmission model that allows a compact notation of all four systems, see, e. g. , [3], [14]. Throughout this paper vectors are defined as column vectors.

2.1. SISO-OFDM and SISO-MC-CDM

In an OFDM system, the available bandwidth W is divided into N subchannels (subcarriers) allowing N symbols to be transmitted simultaneously. The orthogonality between the subcarriers is obtained by adding a cyclic prefix to the transmitted vector. If the length of the cyclic prefix is greater than or equal to the length of the channel impulse response (CIR) each of the subchannels experiences flat fading even if the original channel is frequency-selective. In the following, we assume a time-invariant multipath channel using a T-spaced model of L taps with CIR $\underline{h}_{\mathrm{ch}} = [h_0, \ldots, h_{L-1}]^T$. Furthermore, the length of the cyclic prefix shall be as large as the length of the CIR. Through the use of the inverse discrete Fourier transform (IDFT) and the discrete Fourier transform (DFT), modulation and demodulation can be implemented efficiently. Fig. 1 (left) shows a compact, discrete-time SISO-OFDM matrix-vector model in the frequency domain. The vector $\underline{x}[k]$ represents the OFDM

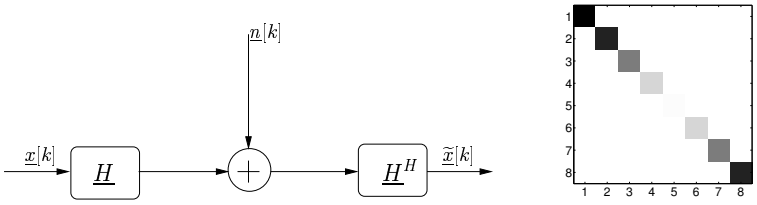

Fig. 1. SISO-OFDM matrix-vector model and example of a SISO-OFDM channel matrix $\underline{R}_{\mathrm{SO}}$.

symbol of size N at time k. Its elements are taken from the M-ary modulation alphabet $\mathcal{A}_x = \{a_1, \ldots, a_M\}$ that may be complex-valued. The $N \times N$ diagonal matrix $\underline{H}$ contains the frequency response of the channel. $\underline{H}$ is given by:

$$\underline{H} = \underline{\mathrm{diag}}(\mathrm{DFT}(\underline{h})), \tag{1}$$

where $\underline{h} = [\underline{h}_{\mathrm{ch}}^T, 0, \ldots, 0]^T$ is the zero padded CIR of length N and "$\underline{\mathrm{diag}}$" stands for composing a diagonal matrix. The vector $\underline{n}[k]$ contains the samples of an AWGN process. Its component variances are given by $\sigma_n^2 = N_0$. At the receiver, perfect channel state information is assumed. Thus, the phase rotation caused by the channel is compensated by the filter $\underline{H}^H$, where $(\cdot)^H$ denotes the conjugate complex transpose operation. Note that Fig. 1 (left) does not contain the addition/removal of the cyclic prefix that results in a loss in SNR. We consider its influence by adapting the noise power.

The received OFDM symbol may also be obtained by:

$$\widetilde{\underline{x}}[k] = \underline{R}_{\mathrm{SO}}\, \underline{x}[k] + \widetilde{\underline{n}}[k], \tag{2}$$

where the discrete-time, diagonal, channel matrix $\underline{R}_{\mathrm{SO}}$ of the SISO-OFDM system is given by:

$$\underline{R}_{\mathrm{SO}} = \underline{H}^H \underline{H}. \tag{3}$$

The vector $\widetilde{\underline{n}}[k]$ contains colored noise samples and has the correlation matrix $2\,N_0\,\underline{R}_{\mathrm{SO}}$ for complex-valued or $N_0\,\underline{R}_{\mathrm{SO}}$ for real-valued modulation alphabets, respectively. Since $\underline{R}_{\mathrm{SO}}$ is diagonal, no joint detection (vector detection) is necessary.

Fig. 1 (right) shows an example of $\underline{R}_{\mathrm{SO}}$ with 8 subchannels (the darker the area, the higher the amplitude). The amplitude is normalized and ranges from 0 to 1. The SISO-OFDM system, however, suffers from the possibility of total fading in one of the subchannels, i. e., $H_{ii} \approx 0$, for a particular i (5th subchannel in Fig. 1 right). Thus, coding is always a necessary part of an OFDM system. An alternative is to spread the energy of each of the N transmitted symbols over some or all of the subcarriers to obtain frequency diversity, i. e., using MC-CDM. The matrix-vector model of SISO-MC-CDM is shown in Fig. 2, where $\underline{U}$ denotes a $N \times N$ spreading matrix. Although intersubchannel interference (ISCI) is introduced through spreading, it may be mitigated through adequate equalization. The channel matrix $\underline{R}_{\mathrm{SM}}$ of the SISO-MC-CDM system is given by:

$$\underline{R}_{\mathrm{SM}} = \underline{U}^H\, \underline{R}_{\mathrm{SO}}\, \underline{U}. \tag{4}$$

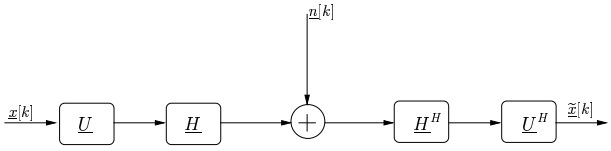

Fig. 2. SISO-MC-CDM matrix-vector model.

2.2. MIMO-OFDM and MIMO-MC-CDM

In the following, we consider a MIMO channel with n_T transmit and n_R receive antennas. The $N \times (n_T\, N)$ MIMO-OFDM matrix for the ith receive antenna $\underline{H}_i$ is defined as $\underline{H}_i = [\underline{H}_{i,1}, \ldots, \underline{H}_{i,n_T}]$. The submatrices $\underline{H}_{i,j}$ are $N \times N$ diagonal matrices and given by:

$$\underline{H}_{i,j} = \underline{\mathrm{diag}}(\mathrm{DFT}(\underline{h}_{ij})), \tag{5}$$

where $\underline{h}_{ij}$ is the zero padded CIR of length N between transmit antenna j ($j = 1, \ldots, n_T$) and receive antenna i ($i = 1, \ldots, n_R$). Accordingly, the discrete-time channel matrix $\underline{R}_{\mathrm{MO}}$ of the MIMO-OFDM system has dimension $(N\, n_T) \times (N\, n_T)$ and is given by:

$$\underline{R}_{\mathrm{MO}} = \sum_{i=1}^{n_R} \underline{R}_{\mathrm{MO},i} = \sum_{i=1}^{n_R} \underline{H}_i^H\, \underline{H}_i. \tag{6}$$

Since $\underline{R}_{\mathrm{MO}}$ is actually a sum of n_R channel matrices, each corresponding to one receive antenna, zero elements on the main diagonal become unlikely by increasing n_R. Fig. 3 shows an example of a MIMO channel with $n_T = n_R = 4$ and the

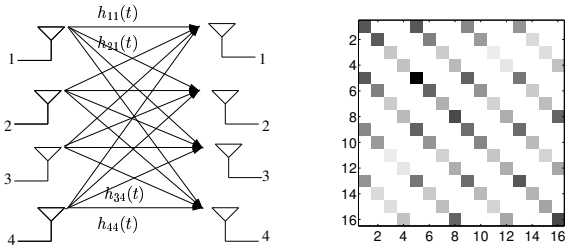

Fig. 3. 4x4 MIMO system model and the corresponding MIMO-OFDM channel matrix $\underline{R}_{\mathrm{MO}}$.

corresponding MIMO-OFDM channel matrix $\underline{R}_{\mathrm{MO}}$. In the frequency domain, four subcarriers ($N = 4$) are available to each of the transmit antennas and are the same for all antennas. The subchannels in Fig. 3 are arranged such that the first four subchannels (rows) correspond to the four subcarriers (frequencies) of the first transmit antenna, the next four subchannels to the second transmit antenna and so forth. Thus, the MIMO-OFDM system model can be thought of as a composition of four SISO-OFDM systems that are transmitting at the same time, while using the same frequencies. The difference lies in the fact that interference occurs due to multiple transmit antennas as visualized in Fig. 3, and in that cooperation at the receive side is possible.

Similar to the SISO-MC-CDM case, symbols of the MIMO-OFDM system may also be spread over several or all of the available subcarriers. The channel matrix in this case is, again, calculated using (4) (and replacing $\underline{R}_{\mathrm{SO}}$ by $\underline{R}_{\mathrm{MO}}$) and the matrix-vector model shown in Fig. 2 is still valid. Fig. 4 depicts the MIMO-MC-CDM channel matrix, $\underline{R}_{\mathrm{MM}}$, corresponding to $\underline{R}_{\mathrm{MO}}$ shown in Fig. 3. The spreading was done at each transmit antenna and over all four subcarriers. The spreading matrix,

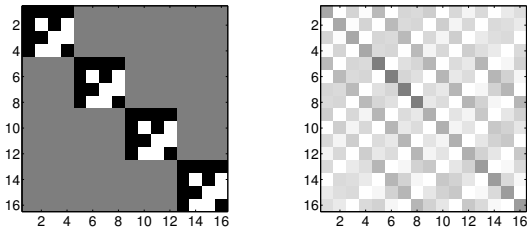

Fig. 4. MIMO spreading matrix (left) and corresponding MIMO-MC-CDM channel matrix $\underline{R}_{\mathrm{MM}}$ (right).

composed of Hadamard matrices, is also shown in Fig. 4 (Note that for spreading matrices the gray areas represent zeros, black are '1' s and white '-1' s). Note that no spatial spreading is applied (over transmit antennas) as indicated by the gray squares. The aim of spreading in MIMO-MC-CDM systems is not to overcome zero diagonal elements, but to equally distribute the symbol energy over the subcarriers. This advantage becomes obvious by looking at the main diagonal elements of the channel matrices. As shown in Fig. 5, the main diagonal elements of $\underline{R}_{\mathrm{MO}}$ are, in general, not equal, whereas every four neighboring diagonal elements of $\underline{R}_{\mathrm{MM}}$ are identical. This is, however, only true if the spreading is done over all four subcarriers. The

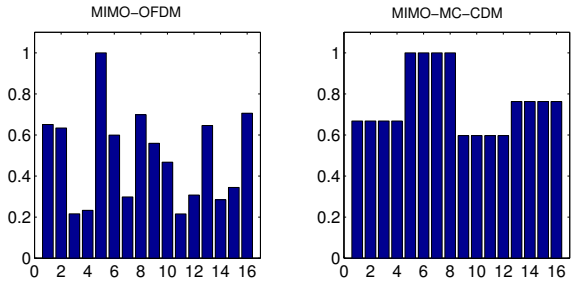

Fig. 5. Normalized diagonal elements of MIMO-OFDM and MIMO-MC-CDM channel matrices.

values of the main diagonal elements influence the matched filter bound (MFB, i. e., all interference is removed perfectly). If all elements were equal, the MFB BER curve would coincide with the AWGN curve. In addition, better BER performance can be expected if equalization adequately mitigates the interference.

2.3. Coded Transmission

Fig. 6 (left) depicts the discrete-time vector-matrix model, when additional coding is included. For ease of notation the time index k is omitted. A sequence of bits $\underline{q}$ is encoded with a terminated convolutional code, optionally punctured with

the puncturing matrix $\underline{P}$ and permuted by a random interleaver $\underline{\Pi}$. The code sequence $\underline{c}$ is mapped to the M-ary symbol alphabet $\mathcal{A}_x$. We assume that the symbol vector $\underline{x}$ is subdivided into blocks of length $N \cdot n_T$, which are transmitted over the discrete-time MIMO channel matrix in parallel. $\underline{R}$ denotes either the channel matrix $\underline{R}_{\mathrm{MO}}$ for MIMO-OFDM or $\underline{R}_{\mathrm{MM}}$ for MIMO-MC-CDM as introduced above. The receive algorithms are briefly discussed in Section 3.

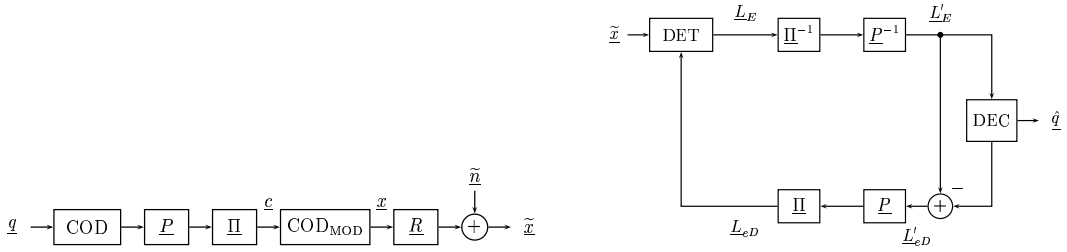

Fig. 6. Matrix-vector model with coding and principle of iterative detection and decoding.

3. Joint Detection Techniques

As mentioned in Section 2, joint detection is required for both MIMO-OFDM and MIMO-MC-CDM to overcome the interference. In the following, we consider two iterative soft interference cancellation schemes. The basic idea of both schemes, the RNN detector [6] and the SCE [10], is to estimate the interference (represented by off-diagonal elements of the channel matrix $\underline{R}$) and subtract it during an iterative process. The difference between the RNN detector and the SCE lies in the soft decision function and an additional preprocessing step of the SCE. The soft decision function of the RNN detector processes a single symbol, whereas the SCE makes a decision based on the whole symbol vector. Furthermore, the SCE applies a whitening filter as preprocessing step in order to reduce the interference. Therefore, the SCE usually offers better performance. However, computational complexity of the SCE is higher compared to the RNN detector. We apply the RNN detector with serial update and the variance computation as defined in [7]. The SCE is used as described in [10].

In the coded case, we apply iterative detection and decoding (turbo detection). The basic principle of turbo detection is depicted in Fig. 6 (right). It was introduced first for ISI channels in [15]. The detector (DET) and the decoder (DEC, BCJR algorithm) benefit from each other during an iterative process by the exchange of soft values (L-values) of the code bits. The output of the detector is deinterleaved ($\underline{\Pi}^{-1}$), depunctured ("$\underline{P}^{-1}$"), and fed to the decoder. The extrinsic output of the decoder is fed back to the detector after puncturing and interleaving. In [15], the optimum APP equalizer was used. Since its computational complexity would be much too large for the scenarios we consider here, we apply the RNN detector and SCE instead as described in [8],[9] and [11]. The performance of the turbo scheme may be enhanced for higher modulation alphabets when additionally IDEM (iterative demapping) for non-Gray mappings is included [13]. We apply this technique for the SCE. Tables I and II depict the mappings for 4 ASK and 8 QAM, respectively. In the case of 4 ASK we use IDEM with natural mapping, for the schemes without IDEM Gray mapping is applied.

TABLE I
MAPPINGS FOR 4 ASK.

symbols	-3	-1	1	3
Gray	00	10	11	01
natural	00	01	10	11

TABLE II
MAPPING FOR 8 QAM.

symbols	$1+\mathrm{j}$	$-1+\mathrm{j}$	$-1-\mathrm{j}$	$1-\mathrm{j}$	$1+\sqrt{3}$	$(1+\sqrt{3})\mathrm{j}$	$-1-\sqrt{3}$	$(-1-\sqrt{3})\mathrm{j}$
bits	100	111	001	010	000	110	101	011

4. Simulation Results

In this section, we show BER simulation results for MIMO-OFDM and MIMO-MC-CDM. As modulation alphabets we use BPSK, 4 ASK, 4 PSK, and 8 QAM. We choose a 4×4 MIMO channel, where the CIR from each transmit to each receive antenna is time-invariant and has length $L = 2$. The channel coefficients are complex-valued, randomly chosen, and kept constant during the whole simulation. The underlying OFDM system has $N = 4$ subcarriers and thus the loss in SNR may be evaluated as $\gamma = 10\log_{10}(\frac{N+L-1}{N}) \approx 0.97\,\mathrm{dB}$. We note that we considered this small OFDM system only, since it suffices to obtain essential properties in a MIMO environment. However, in practice a much larger number of subcarriers would be used. For MIMO-MC-CDM spreading over all four subcarriers with a 4×4 Hadamard matrix is applied. In a practical system with more subcarriers spreading should be adapted so that a trade-off between diversity and complexity is obtained. The channel matrices of both systems are depicted in Figs. 3 and 4. For the coded case, the convolutional code is rate $\frac{1}{2}$ with memory 2 and generator polynomials $[7\ 5]_8$. The length of one codeword is adapted to the symbol alphabet resulting in $100\,N\,n_T = 1600$ transmit symbols. We apply a random interleaver which has the length of one codeword. The detection schemes under consideration are the linear MMSE detector [16], the RNN detector and the SCE. In the uncoded case, we use

5 iterations for the SCE and 10 iterations for the RNN, whereas in the coded case 10 iterations (10 detection and 10 decoding steps) are used for both turbo schemes.

In Fig. 7 (a) to (c), the BER curves for uncoded transmission for BPSK, 4 PSK, and 4 ASK and the MIMO-OFDM and MIMO-MC-CDM channel matrices given in Section 2 are shown. In the case of BPSK and 4 ASK, only the real part of the channel matrix and the received vector were used. That is, the 4 PSK transmission scheme sees a complex channel, while the other transmission schemes see a real one. The eigenvalues of the complex channel matrix are in general different from those of just its real part and in this case 4 ASK outperforms 4 PSK. As reference, the AWGN OFDM BER curves for each of the given transmission schemes as well as the MFB are shown. Gray mapping is assumed for all transmission schemes.
As expected, the MFB in the case of MC-CDM lies closer to the AWGN curve and is around 2 dB better that the OFDM MFB in all cases. At low SNR, MIMO-OFDM and MC-CDM perform equally. At higher SNR, the MIMO-MC-CDM transmission leads to better BERs for the linear MMSE detector and SCE. More than 2 dB improvement is observed by the linear MMSE detector in the case of BPSK and around 1 dB improvement in the case of the SCE for BPSK, 4 PSK and 4 ASK. The RNN detector does not converge to a low BER and has the worst performance for 4 ASK. This can be explained by the fact that the RNN does not have a whitening filter like the SCE that reduces interference significantly.

In the coded case, we use sequential detection and decoding (one detection step, one decoding step) when applying the linear MMSE detector and turbo detection for the SCE and the RNN detector. In Fig. 7 (d) to (f) the results for the coded transmission are depicted. Again, we observe that MIMO-MC-CDM performs better than MIMO-OFDM for BPSK. Furthermore, we obtain better results with the RNN detector than with the linear MMSE detector through the use of iterative detection and decoding. For 4 ASK (e) and 8 QAM (f) the interference is too strong, therefore the RNN detector shows an error floor. In these cases, the error floor is lower for MIMO-OFDM, since there is less interference than for MIMO-MC-CDM. However, when using the linear MMSE detector and SCE MIMO-MC-CDM outperforms MIMO-OFDM. Additionally, for 4 ASK and 8 QAM the AWGN IDEM reference curves (dashed lines) are depicted. In the case of 4 ASK the performance of the SCE is improved for high SNR by including IDEM in the turbo scheme and applying natural mapping. For low SNR natural mapping performs worse than Gray mapping (also indicated by the corresponding AWGN curves). However, the advantage of IDEM is more obvious for the 8 QAM constellation, where there is no need to change the type of mapping [13]. Here, we observe an improvement of 2 dB for BER of $2 \cdot 10^{-4}$ over conventional turbo detection without IDEM.

5. Conclusions

We investigated a MIMO-OFDM system in conjunction with spreading over subcarriers (MIMO-MC-CDM) and several iterative detection schemes. It is shown that the same matrix-vector model used for the SISO-OFDM/SISO-MC-CDM case can also be applied to MIMO-OFDM/MIMO-MC-CDM. For nearly all detection schemes the simulation results show that MIMO-MC-CDM performs better than MIMO-OFDM. Furthermore, we observe that the SCE is a suitable detection scheme for this transmission method where intercarrier interference is the main problem. Future work will include the extension of the transmission scheme to a larger number of subcarriers and the investigation of spreading over antennas, see, e. g. , [17].

References

[1] N. Yee, J. P. Linnartz, and G. Fettweis, "Multicarrier CDMA in indoor wireless radio networks," in *Proc. PIMRC*, 1993, pp. 975–979.

[2] K. Fazel and G. Fettweis, *Multi-Carrier Spread Spectrum*. Kluwer Academic Publishers, The Netherlands, 1997.

[3] J. Lindner, "MC-CDMA in the context of general multiuser/multisubchannel transmission methods," *European Trans. Telecomm.*, vol. 10, no. 5, pp. 351–367, July/Aug. 1999.

[4] G. J. Foschini and M. J. Gans, "On limits of wireless communications in a fading environment when using multiple antennas," *Wireless Personal Commun.*, vol. 6, no. 3, pp. 311–335, Mar. 1998.

[5] W. G. Teich and M. Seidl, "Code division multiple access communications: Multiuser detection based on a recurrent neural network structure," in *Proc. IEEE ISSSTA*, vol. 3, Mainz/Germany, Sept. 1996, pp. 979–984.

[6] C. Sgraja, A. Engelhart, W. G. Teich, and J. Lindner, "Equalization with recurrent neural networks for complex-valued modulation schemes," in *Proc. 3rd Workshop Kommunikationstechnik*, Reisensburg/Germany, June 1999.

[7] ——, "Multiuser/multisubchannel detection based on recurrent neural network structures for linear modulation schemes with general complex-valued symbol alphabet," in *Proc. COST 262 Workshop on Multiuser Detection in Spread Spectrum Communications*, Reisensburg/Germany, Jan. 2001, pp. 45–52.

[8] ——, "Combined equalization and decoding for BFDM packet transmission schemes," in *Proc. 1st Int. OFDM-Workshop*, Hamburg/Germany, Sept. 1999, pp. 19–1ff.

[9] M. A. Dangl, J. Egle, C. Sgraja, W. G. Teich, and J. Lindner, "Convergence of RNN based iterative equalization and decoding," in *COST 262 MCM meeting*, TD 068(02), Prague/Czech Republic, Sept. 2002.

[10] J. Egle, C. Sgraja, and J. Lindner, "Iterative soft cholesky block decision feedback equalizer – a promising approach to combat interference," in *Proc. IEEE VTC*, vol. 3, Rhodes/Greece, May 2001, pp. 1604–1608.

[11] J. Egle and J. Lindner, "Iterative joint equalization and decoding based on soft cholesky equalization for general complex valued modulation symbols," in *Proc. 6th Int. Symposium on DSP for Communication Systems*, Sydney-Manly/Australia, Jan. 2002, pp. 163–170.

[12] S. ten Brink, J. Speidel, and R. Yan, "Iterative demapping and decoding for multilevel modulation," in *Proc. IEEE GLOBECOM*, Sydney/Australia, Nov. 1998, pp. 579–584.

[13] M. A. Dangl, W. G. Teich, J. Lindner, and J. Egle, "Joint iterative equalization, demapping, and decoding with a soft interference canceler," in *Proc. Int. Symp. on Commun. Theory and Appl.*, Ambleside/UK, July 2003, accepted for publication.

[14] J. Lindner and C. Pietsch, "The spatial dimension in the case of MC-CDMA," *European Trans. Telecomm.*, no. 5, pp. 431–438, Sept./Oct. 2002.

[15] C. Douillard, M. Jezequel, C. Berrou, A. Picart, P. Didier, and A. Glavieux, "Iterative correction of intersymbol interference: Turbo-equalization," *European Trans. Telecomm.*, vol. 6, no. 5, pp. 507–511, Sept./Oct. 1995.

[16] S. Verdú, *Multiuser Detection*. Cambridge University Press, 1998.

[17] C. Pietsch, S. Sand, W. G. Teich, and J. Lindner, "Modeling and performance evaluation of multiuser MIMO systems using real-valued matrices," *IEEE Journal on Selected Areas in Communications*, June 2003, to appear.

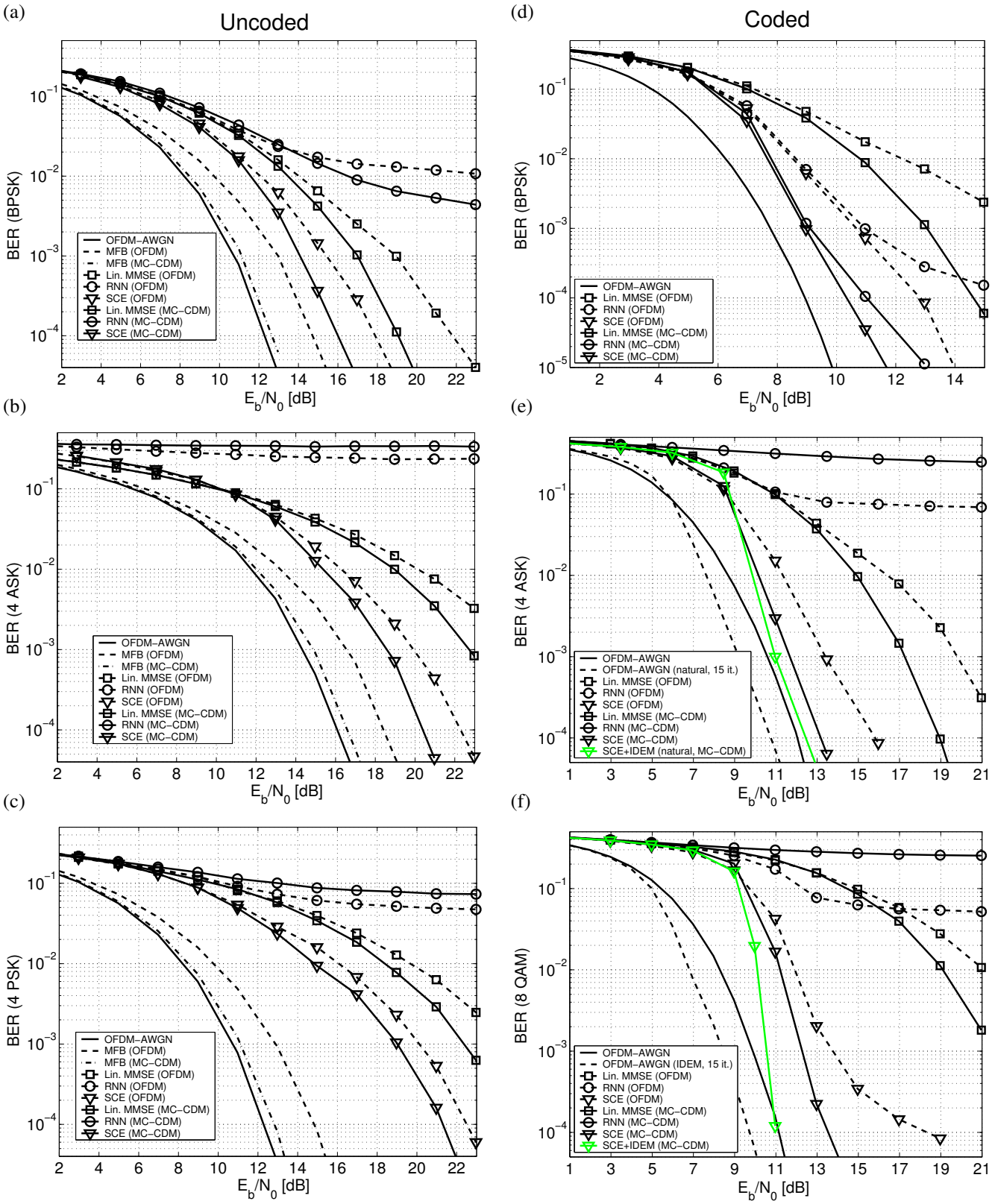

Fig. 7. BER of joint detection schemes, 4×4 time-invariant MIMO channel (details see text): uncoded BPSK (a), uncoded 4 ASK (b), uncoded 4 PSK (c), coded BPSK (d), coded 4 ASK (e), and coded 8 QAM (f). Convolutional code is rate $\frac{1}{2}$ with memory 2 and generator polynomials $[7\ 5]_8$.

Sponsors

SAGEM

European Commission

Délégation Générale pour l'Armement

FRANCE TELECOM R&D

MITSUBISHI Electric ITE
Centre de Rennes